JOURNAL OF GEOPHYSICAL RESEARCH, VOL. 105, NO. A10, PAGES 23,263–23,276, OCTOBER 1, 2000

Study of weak substorms observed during December 8, 1990, Geospace Environment Modeling campaign: Timing of different types of substorm onsets

V. M. Mishin
Institute of Solar-Terrestrial Physics, Russian Academy of Sciences, Irkutsk

C. T. Russell
Institute of Geophysics and Planetary Physics, University of California, Los Angeles

T. I. Saifudinova and A. D. Bazarzhapov
Institute of Solar-Terrestrial Physics, Russian Academy of Sciences, Irkutsk

Abstract. We define an expansion onset (synonymous with the main breakup) to be one with sufficient signatures of open tail reconnection. Earlier onsets, which we term initial onsets, occur before the expansion onset, without the signatures of open tail reconnection but with other signs of a clear substorm onset. These two types of substorm onsets and their timing are discussed herein in a study of selected substorm-like events. During the 10-hour interval studied, five impulses of the Perreault-Akasofu index ε were observed with comparable peak values. However, the observed magnetospheric responses were very different in terms of equatorward motion and poleward expansion of the auroral oval. We conclude that the occurrence either of an initial onset or of a full onset (under similar boundary conditions) depends on the amount of stored free energy, proportional to the tail length, which is controlled by the input power. The earlier or initial onset marks a sudden change in the convection pattern in the nightside. This onset could mark the initiation of reconnection on closed field lines while the expansion onset could mark the initiation of reconnection on open field lines.

1. Introduction

It is conventional wisdom that in the early 1970s the number of substorm models was approximately equal to the number of theorists working in this field. Since then the number of theorists has increased and the situation still persists. Indeed, while the classical Near-Earth neutral line (NENL) model [*Russell and McPherron*, 1973] retains its position [*Baker et al.*, 1996; *Birn et al.*, 1996], models with small-scale current disruptions (CDs) in the innermost plasma sheet have evolved [*Lui*, 1996, and references therein; *Kan*, 1993; *Maynard et al.*, 1996; *Erickson et al.*, 1996], and other new approaches to the substorm have been proposed, both by *Rostoker* [1996 and references therein] and by *Sergeev et al.* [1996]. Added to the great diversity of substorm models is the fact that in the current literature each of the key terms, "substorm," "expansion onset," "pseudobreakup," etc., has different definitions, corresponding to different models and concepts. Despite the diversity of approaches, it is possible to recognize two major types of substorm models. The first includes current instabilities or current disruptions in the innermost current sheet, with or without magnetosphere-ionosphere coupling. The second involves open tail reconnection in the middle tail (NENL model). Some authors, following *Rothwell et al.* [1988] and *Lui* [1991], seek to synthesize both approaches, assuming a leading role for the CD processes. On the other hand, according to others such as *Baker et al.* [1996] and *Pulkkinen et al.* [1998a, b], only open flux reconnection is of fundamental significance, because the energy to feed the substorm processes in both the middle and near-Earth tail is stored in the open tail region.

Hence one of the tasks of each substorm case study is to distinguish in time and space, and/or by physical signatures, the two principal above mentioned processes for creating the substorm, i.e., with and without open tail reconnection. It is now possible to do that, because of new information on the variation of the open tail magnetic flux Ψ_1, as discussed in section 2. Such an approach determines the general goals of this study. The timing and description of the substorm-like events on December 8, 1990, are performed using a traditional substorm method supplemented by data from the magnetogram inversion technique (MIT-2), including a plot of the $\Psi_1$variation, and plots of other special parameters, calculated on the basis of Ψ_1. These special parameters and slightly updated definitions of the above mentioned key terms are given in sections 2 and 3, respectively, to provide the unfamiliar reader with a quick and efficient introduction to the MIT-2 technique and the corresponding, developing, substorm scenario. The database and results of the study are described in section 4. Section 5 is devoted to the discussion and conclusions. On the whole, the problem of timing the onsets of substorm phases and also the corresponding duration of the principal phases of typical substorms is addressed in this paper. The results are tested and applied to the study of selected, weak, overlapping, winter substorms. Results support a substorm scenario with two active

Paper number 1999JA900495.
0148-0227/00/1999JA900495$09.00

phases without and with open magnetic flux reconnection, respectively, [*Mishin*, 1991; *Mishin et al.*, 1997].

This paper is the first of a series, which will be devoted to the December 8, 1990, events. Sections 2 and 3 of the present paper also serve as introductory material for these other papers of the series.

2. The MIT-2 Parameters

The magnetogram inversion technique (MIT) uses as inputs measurements from the worldwide array of ground-based magnetometers and a carefully selected model of the ionospheric height-integrated anisotropic conductivity. The primary output is a two-dimensional (2-D) spatial distribution of the electric field, Hall, Pedersen, and field-aligned current (FAC) density in a thin conducting sheet at the height of the E layer in the high-latitude ionosphere. Additionally, the polar cap boundary is determined, assuming that it coincides with the high-latitude boundary of the region 1 FAC. This allows the determination of the polar cap area S and its magnetic flux Ψ. The flux equals λBS where B is the mean value of the magnetic field across the northern polar cap, S is the polar cap area, and λ is a correction factor ~1, dependent on the length of a series of spherical functions, approximating the current function $J(\Phi,t)$ [*Mishin*, 1990, p. 91]. Using Ψ, in turn, a series of secondary parameters, describing the global magnetospheric electrodynamics, are calculated.

The basic MIT equation is the same as that of the well-known Kamide-Richmond-Matsushita (KRM) method [*Kamide et al.*, 1981]. Derivation of this equation is based upon simplifying assumptions:

1. Only ionospheric and field-aligned currents are considered to be sources of the ground geomagnetic variations; the contributions of the disturbed ring current (DR), magnetopause currents, etc., are neglected.
2. The geomagnetic field lines are assumed radial, which is equivalent to the assumption that the ground magnetic field produced by field-aligned currents and their ionospheric continuation compensate each other [*Fukushima*, 1976, and references therein].

Assumptions 1 and 2 retain only currents closed in the ionosphere as the source of the ground variation field. Therefore the solenoidal current density may be represented as

$$\mathbf{j}^{(s)} = \mathbf{n} \times \nabla_{\perp} J, \tag{1}$$

where $\mathbf{n}$ is the outward normal to the current-carrying ionospheric surface and $J(\Phi,t)$ is the current function unambiguously determined from the magnetic potential of the variation field [*Chapman and Bartels*, 1940].

3. The electric field in the ionosphere is assumed to be a potential field:

$$\mathbf{E}_{\perp} = -\nabla_{\perp} U. \tag{2}$$

The symbol $\perp$ means in the plane perpendicular to the magnetic field $\mathbf{B}$. The operator $\nabla_{\perp}$ denotes that only derivatives perpendicular to B are taken.

With provision for assumptions 1-3, let the vector of ionospheric current density $\mathbf{j}$ be represented as the sum of the solenoidal and the potential parts,

$$\mathbf{j}_{\perp} = \mathbf{n} \times \nabla_{\perp} J + \nabla_{\perp} \theta, \tag{3}$$

and using Ohm's law,

$$\mathbf{j}_{\perp} = -\hat{\Sigma}_{\perp} U \tag{4}$$

where the magnetic potential θ is an arbitrary scalar and $\hat{\Sigma} = \hat{\Sigma}(\Phi,t)$ is the two-dimensional ionospheric conductivity tensor. From (3) and (4) in a Cartesian coordinate system, x, y and z, we have

$$\nabla \times (\hat{\Sigma}\ \nabla_{\perp} U) = -\nabla_{\perp}^2 J. \tag{5}$$

and the corresponding equation in spherical geomagnetic coordinates, Φ (latitude) and t (local time).

With the function $\hat{\Sigma}(\Phi,t)$ and $J(\Phi,t)$ specified, the basic equation (5) in spherical geomagnetic coordinates is solvable for the electric potential $U(\Phi,t)$. The boundary conditions in this case are those for which the electric potential at the poles is zero as well as the derivative $\partial U/\partial\Phi$ at the equator.

The MIT-0 variant [*Mishin*, 1968] corresponds to the simplest spatial model of ionospheric conductivity

$$\hat{\Sigma}(\Phi,t) = const. \tag{6}$$

In this case, assuming

$$j_{\parallel} = -\nabla_{\perp} \mathbf{j}_{\perp}, \tag{7}$$

from (5) we have

$$j_{\parallel} = (\Sigma_P/\Sigma_H)\nabla_{\perp}^2 J, \tag{8}$$

$$U = J/\Sigma_H. \tag{9}$$

The MIT-1 variant takes into account the ionospheric conductivity inhomogeneity. For this purpose, *Mishin et al.* [1980] used a statistical model, which describes the distribution of $\Sigma(\Phi,t)$ averaged over years. It did not allow variability of conductivity to be taken into account. *Mishin et al.* [1983, 1986] used an instantaneous model by adapting a statistical model [*Spiro et al.*, 1982] to a given moment of universal time.

During substorms the spatial pattern of the electric potential, calculated by MIT taking the actual spatial inhomogeneity of the ionosphere into account, differs even qualitatively from that corresponding to uniform conductivity [e.g., *Kamide and Richmond*, 1982]. However, many years of experience in the case of the magnetogram inversion technique show that the position of the FAC Region 1 boundary virtually does not change in going (in MIT calculations) from one conductivity model to another reasonably chosen model. In practice, therefore, it is possible to use a spatially homogeneous conductivity model when determining the polar cap boundary. The location of the polar cap boundary in this case coincides with that for the inhomogeneous conductivity case within 1°-3° of latitude; polar cap areas for the above mentioned conductivity models coincide within $\pm 10\%$. Thus, irrespective of the ionospheric conductivity model used, errors in determining the polar cap area turn out to be rather small; they lie within those of the more direct methods (see, e.g., Figure 1. The main reason for these relatively small errors is perhaps that the most significant FACs appear near or at the electrojets, which give the clearest signatures on the ground. Thus quantitative errors in FAC density can be large, but location errors are small.

MIT-2 is an extension of MIT which enables the determination of the polar cap boundary assuming that it coincides with the

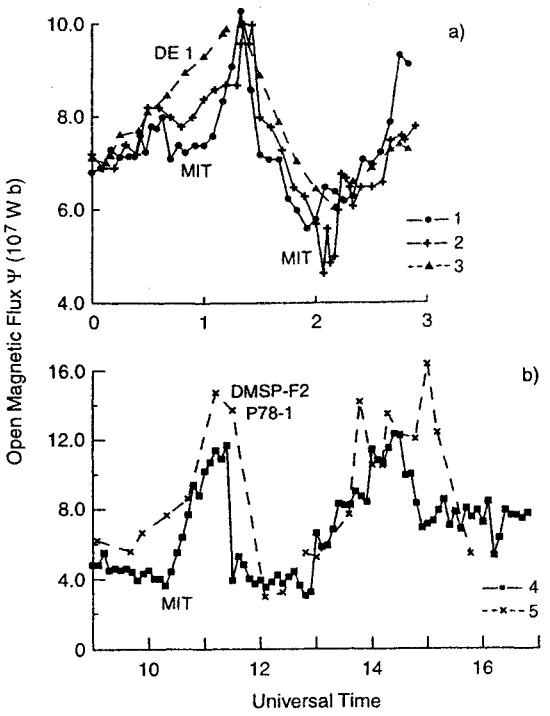

Figure 1. Variations of the magnetic flux through the polar cap (Ψ) in the course of two substorms: (a) May 3, 1986, 0000-0300 UT and (b) March 22, 1979, 0900-1700 UT. 1 and 4, magnetogram inversion technique (MIT) data, spectrum of spherical harmonics: n = 26, m = 4; 2, MIT data, spectrum of spherical harmonics: n = 40, m = 4; 3, DE 1 data [Baker et al., 1994]; 5, DMSP-F2 and P78-1 data [Holzer et al., 1986].

high-latitudinal boundary of FAC Region 1 [*Mishin*, 1990; and references therein]. Thus MIT-2 allows one to find an improved polar cap area S and the polar cap magnetic flux Ψ and as before a set of secondary parameters relevant to the electrodynamics of the magnetosphere. The main conclusions reported in this paper are drawn on the basis of MIT-2 data. These conclusions do not depend much on the ionospheric conductivity model used. This claim has been confirmed by the series of tests described below.

To estimate the MIT-2 errors, *Mishin et al.* [1992] compared results of the MIT-2 method of the determination of the polar cap boundary both with statistical results of an independent method by *Elphinstone et al.* [1991], who used Viking auroral images, and with the results by *Birn et al.* [1991], who used the Tsyganenko 1987 model. In both cases the polar cap boundaries obtained by two methods did not differ more than by 1°-3° of latitude. Figure 1a shows the third comparison with DE 1 auroral images [*Baker et al.*, 1994]. This gave a worse but still satisfactory result. In Figure 1a the variations of the magnetic flux through the northern polar cap area (S), are shown in the course of a substorm from 0000 to 0300 UT, on May 3, 1986, as obtained by two methods. One can see that the greatest discrepancy of the two methods does not exceed 21% for the lower-order spectrum of spherical functions approximating the current function $J(\Phi,t)$ and 13% for the higher-order spectrum. Note that the maxima of Ψ on the three plots in Figure 1a coincide in time. That characteristic is most important for timing the substorm phases. Similar results are shown in Figure 1b for the Coordinated Data Analysis Workshop 6 (CDAW6) substorm of March 22, 1979. We now discuss each of the major parameters determined by MIT-2.

2.1. Polar Cap Magnetic Flux Ψ

As mentioned above, the polar cap magnetic flux is given by

$$\Psi = \lambda BS \tag{10}$$

for one hemisphere. Magnetic flux Ψ is conserved in the tail, so that the equation

$$\Psi = B_T S_T \tag{10'}$$

also holds approximately, where B_T and S_T are, respectively, the magnetic field and summed cross section of one tail lobe. The numerical value of S_T will be specified in section 2.2.

2.2. Polar Cap Flux $\Psi 2$

The polar cap flux Ψ_2 is the value of Ψ at the quietest conditions prior to the substorm under study, when the Perreault-Akasofu index $\varepsilon \rightarrow 0$ [*Perreault and Akasofu*, 1978]. For more active periods we can then write

$$\Psi = \Psi_1 + \Psi_2 \tag{11}$$

where Ψ_2 corresponds to the above reference level and $\Psi_1$is the excess polar cap flux accompanying the higher activity. Figure 2 gives a typical example of a Ψ plot for a time interval containing both quiet and substorm periods. One can see significant flux Ψ ($\sim 4 \times 10^8$ Wb) even at the most quiet time (before 2045 UT) when the Perreault-Akasofu index $\varepsilon \rightarrow 0$. The Ψ values increase during substorms by a factor of 2-3, at most, as seen in Figure 2. For the other examples, see, for example, *Stern and Alexeev* [1988], *Petrinec and Russell* [1996], and *Sotirelis et al.* [1998]. The values of Ψ_1 and Ψ_2 are associated with the variable part of the polar cap and its near-pole part that remains at quiet times, respectively. The spatial distribution of Ψ_1 and Ψ_2 in the tail is unknown. Moreover, the magnetic flux density and cross section of the tail vary during substorms and with distance from the Earth [*Petrinec and Russell*, 1996]. We assume for both fluxes the same cross section S_T, that is,

$$\Psi_1 = B_{T1} S_T;\ \Psi_2 = B_{T2} S_T,$$

although these equations will not be used to calculate B_{T1} and B_{T2} with Ψ_1, Ψ_2, and S_T given.

We use the Perreault-Akasofu index because of its common use in substorm studies and because it attempts to predict the energy flux into the magnetosphere solely on the basis of solar wind data without reference to magnetospheric data. The original *Dungey* [1961] model transferred mechanical energy of the solar wind into the magnetosphere through reconnection. In this process the solar wind slows down as it stretches the newly connected tail field and adds flux to the magnetotail. The addition of magnetic flux to the tail constitutes a Poynting flux of energy into the magnetotail, but this energy is extracted from the flowing solar wind plasma so that the integrated momentum flux of the solar wind is reduced on those streamlines that intersect the region close to the magnetopause. As discussed in section 2.3, we can estimate this Poynting flux from magnetospheric information. *Perreault and Akasofu* [1978] used a different approach, based on the assumption that the magnetosphere absorbs directly the

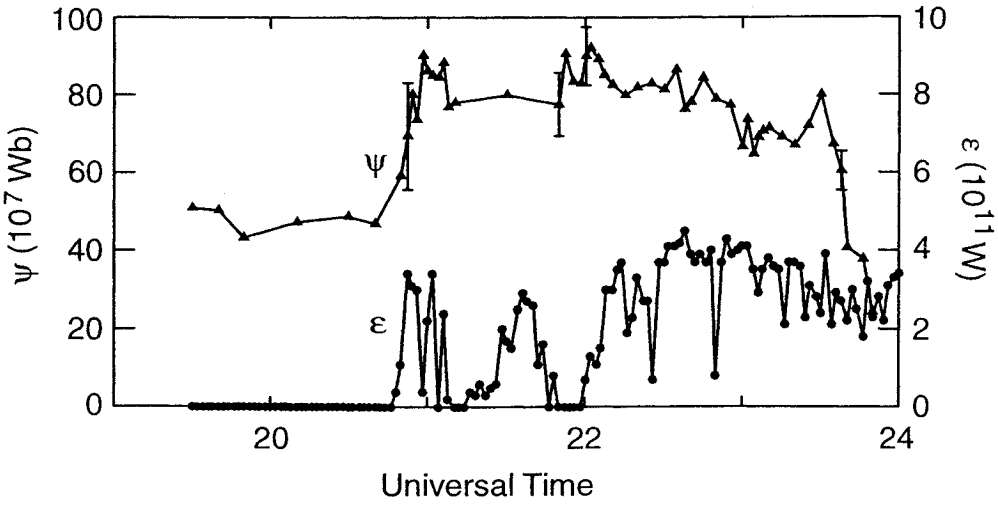

Figure 2. Illustration of the method of determining Ψ_2. In this example, Ψ_2 is the average value of Ψ observed before the start of the substorm at 2045 UT, September 25, 1986, under quiet conditions when the Perreault-Akasofu index $\varepsilon \rightarrow 0$.

Poynting flux of the solar wind without tapping the mechanical energy flow, with a fixed geometric window for this energy flow and an efficiency controlled by the interplanetary magnetic flux (IMF) direction. *Burton et al.* [1975a] had earlier shown empirically that the energy flow into one of the magnetospheric energy reservoirs, the ring current, was proportional to the southward magnetic flux convected against the magnetosphere, i.e., the dawn-dusk electric field. In the *Burton et al.* model it is the amount of reconnected magnetic field that taps the solar wind momentum flux and energizes the magnetosphere and not the incident Poynting flux per se. However, we use the Perreault-Akasofu index only qualitatively. Moreover, the arbitrarily chosen $\sin^4\theta/2$ angular dependence in the Perreault-Akasofu model is similar to that found in quantitative geomagnetic studies [*Scurry and Russell*, 1991] and not much different from the half-wave rectifier of *Burton et al.* [1975b]. Thus, for our purpose of monitoring the energy flow that is available for geomagnetic activity, the ε parameter seems to be satisfactory.

2.3. Poynting Vector Flux

The Poynting flux from the solar wind into the magnetotail is the next parameter derived from the MIT-2 data together with the solar wind velocity data of ISEE 3 or IMP 8. We estimate this from the rate of change of energy stored in the tail. It is a secondary parameter that will be compared with another qualitative estimate of solar wind Poynting flux into the magnetosphere of Perreault and Akasofu. Thus the fact that we cannot accurately measure the tail Poynting flux from the MIT-2 parameters does not affect our interpretation below, although it does reinforce what we conclude.

The magnetic energy in the tail is the integral of the magnetic field energy density ($B^2/2\mu_0$) over the volume of the tail. For our purposes we are interested in the volume that can be tapped for substorm energization. We assume that the quiet time flux Ψ_2 does not participate in the substorm process, and we need only consider Ψ_1. We also assume that energy storage occurs principally through a lengthening of the storage region rather than an increase in the energy per unit length of the tail. Then we can write that

$$\varepsilon' = \Psi_1^2 V /(\mu_0 S_T), \tag{12}$$

where $\mu_0 = 4\pi 10^{-7} H\, m^{-1}$, V, is the solar wind speed, and S_T is the cross section of one magnetotail lobe, containing the variable open flux (Ψ_1) that is given by

$$\Psi_1 = BT_1 ST. \tag{13}$$

Indeed, the Poynting flux, or the energy flux, into the lobe magnetic field of a lengthening tail is

$$\varepsilon' = W_B S_T V', \tag{14}$$

where V' is the speed of the magnetic energy density which coincides approximately with the speed of the lengthening of the tail, assumed to be equal to half of the solar wind velocity,

$$V = 2V', \tag{15}$$

and W_B is the energy density of the open tail magnetic field,

$$W_B = B_{T_1}^2 / 2\mu_0. \tag{16}$$

Taking (15), (16), and (13), we have (12) from (14).

Equation (13) requires additional comments. To specify the value of S_T, we use $S_T = \pi R_T^2 / 2$, with $R_T = 22.5\ R_E$, which ensures the approximate equality of long-time average values of ε' and Perreault-Akasofu's proxy index ε, having a similar but not identical value as ε' [*Mishin*, 1990]. Besides, with $R_T = 22.5\ R_E$ we have good agreement of the theoretical and observed values of the "tail length" L; see below in this section. There are other arguments from the analysis of data obtained on the basis of (12), which will be given in section 2.4. Note that R_T is a weakly variable quantity. At $|x| \sim$ 10-20 R_E the magnetotail radius changes during the substorm within ~ 18-25 R_E [*Akasofu*, 1977 and references therein; also *Petrinec and Russell*, 1996]. Therefore, by assuming that R_T is constant we somewhat overestimate the range of variation of ε'.

2.4. Efficiency of Power Generator and "Tail Length" L

The secondary characteristics of the efficiency of power generator and tail length L are calculated in the framework of the 2-D

Dungey model using the MIT parameter Ψ_1 and solar wind parameters measured by a satellite. For this purpose we now consider the continuity equation for the variable open magnetic flux Ψ_1. The difference between the rates of reconnection on the dayside and the tail are [*Russell*, 1980]

$$M\text{-}R = d\,\Psi_1/dt. \tag{17}$$

Here M is the magnetic merging rate at the dayside neutral point N_1; R is the reconnection rate at the nightside neutral point N_2.

Following *Mishin* [1990], suppose that

$$R(t) = M(t - \Delta t), \tag{18}$$

$$\Delta t = L / V', \tag{19}$$

where t is time and L is the "tail length," i.e., the distance between N_1 and N_2. For $t > t_0 + \Delta t$ the flux in one lobe is

$$\Psi_1 = M\,L/\,V' \tag{20}$$

if it is assumed also, for the sake of simplicity, that $M = 0$ when $t < t_0$ and M = const. > 0 when $t > t_0$. From (12) and (20) and accounting for the energy flow into both lobes, it follows that

$$\varepsilon' = M^2L^2/\mu_0\,S_T\,V \tag{21}$$

when it is evident that the input power ε' varies as L^2 when M = const. In other words, the efficiency κ of the power ε'generator is proportional to L^2, i.e.,

$$\kappa = (L/\,L_0)^2, \tag{22}$$

where L_0 is some basic (constant) value. We now recall that the parameter ε' has a similar meaning to that purported for the Perreault-Akasofu index ε. However, that index uses solely solar wind data to calculate the solar wind Poynting flux, assuming that the amount of that flux incident on a fixed area of the dayside of the magnetosphere enters it with an efficiency factor controlled by the IMF orientation. This parameter is defined as

$$\varepsilon = VB^2 \sin^4(\theta/2)\, l_0^2, \tag{23}$$

where l_0 = const. The latter constancy means that (23) implies an invariable geometry and size of geomagnetosphere. Therefore, with $L = L_0$ we may write $\varepsilon = \varepsilon'$, that is,

$$\varepsilon = M^2\,L_0^2/\mu_0\,S_T\,V. \tag{21'}$$

From (21), (22), and (21′) it follows that

$$\kappa = \varepsilon'/\varepsilon, \tag{24}$$

$$(L/\,L_0)^2 = \varepsilon'/\varepsilon. \tag{25}$$

Now, to estimate the theoretical value of L_0, let us use the equation for M from *Kan and Lee* [1979]:

$$M = \sqrt{10^{-7}\varepsilon V}\,. \tag{26}$$

Combining (20), (26), and (25) with $\varepsilon' = \varepsilon$, we have $(L_0)^2 = 4\pi S_T$. With $S_T = \pi R_T^2/2$ and $R_T = 22.5\,R_E$ we find

$$L_0 = 141\,R_E. \tag{27}$$

Since the value of l_0 in (23) is an empirical long-time average value, the value of L_0 is also a long-time average. Thus L_0 is the characteristic value, which "tail length" (a distance between neutral points N_1 and N_2) may be compared with observations. According to *Slavin et al.* [1985], the observed average value of above N_1, N_2 distance is

$$L_0 = 130\,R_E. \tag{28}$$

This estimate, (28), is quite consistent with that of (27), which supports the method described and allows us to use this method for the calculation of L. In this study, the plot of the L variation will be used for substorm timing. Values of the tail length close to 130 R_E or more are signatures that the distant neutral line is acting, without predominant near-Earth open tail reconnection. In contrast, values of L that suddenly decrease to ~40 R_E are the signatures of NENL formation.

2.5. The Tool for Timing: Parameter t_w

From the equivalent current system the location (latitude (Φ_N) and magnetic local time, MLT, (t_w) of the western end of the westward electrojet) can be found. This location coincides with the center of Harang discontinuity in the DP2 current system but not in the DP1 current. The parameters t_w and Φ_N (especially the former) can serve as indicators of the type of equivalent current system: a value of t_w ~23 hours MLT corresponds to a DP2 type, i.e., to a two-vortex current system existing under quiet conditions and in a substorm before the appearance of the current wedge or, equivalently, before the appearance of cross-tail current disruption. The actual system of ionospheric Hall currents is qualitatively identical to the equivalent current system. Therefore the dynamics of the latter qualitatively reflects also the dynamics of the convection system, $\mathbf{E} \times \mathbf{B}$ - drift, of the ionospheric plasma.

Disruption of the cross-tail current produces a current wedge which includes the ionospheric westward electrojet [e.g., *McPherron et al.*, 1973, and references therein]. The superposition of the latter on DP2 currents enhances the preexisting westward auroral electrojet and weakens the eastward one. Thus the overall current system is altered: the morning vortex (containing the westward electrojet) is enhanced, and the eastward vortex is partially suppressed. The system becomes a quasi one-vortex system, which is denoted by the symbol DP1. For an example of the DP2 → DP1 transition described above see Figure 3. Here a "clean" DP2 signature and a "clean" DP1 signature are observed at 0105 and 0140 UT, respectively, on May 3, 1986. It is evident that the DP2 → DP1 transition is characterized by a variation of t_w from ~23 hours MLT to 15.5 hours MLT and by a variation of Φ_N from 61° to 72°. Such variations of t_w and Φ_N are typical of substorms, although their swing varies within 4-8 hours of MLT. (For details, see *Mishin* [1991].) From the foregoing discussion it follows that the DP2 → DP1 transitions characterize the current wedge dynamics. As will be apparent in the following, plots of t_w and Φ_N are used to time substorms, i.e., to determine onset times of the various phases.

The other tool for substorm timing is the difference between power input and internal dissipation:

$$P = \varepsilon' - Q_T. \tag{29}$$

(We use Q_T synonymously with U_T of *Akasofu* [1981] to avoid confusion with universal time (UT). The sign of P is a signature of substorm phase: loading of the tail predominates where P > 0 and unloading predominates when $P < 0$. The total substorm dissipation power was calculated from [Akasofu, 1981]

$$Q_T = 2Q_i + 2Q_A + Q_{DR}. \tag{30}$$

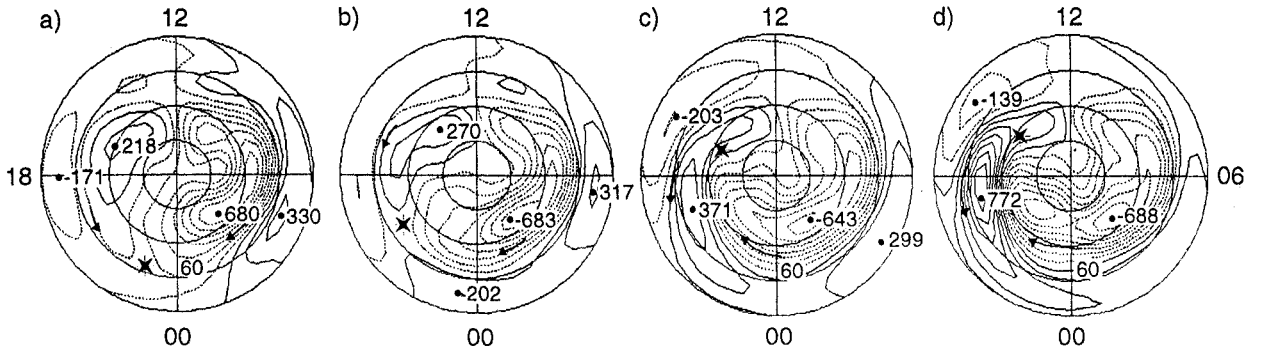

Figure 3. MIT equivalent current systems at the May 3, 1986, Coordinated Data Analysis Workshop 9C-1 (CDAW9C-1) substorm at (a) 0105, (b) 0120, (c) 0135, and (d) 0140 UT. The distance between isocontours is 100 kA. Bold arrows indicate the current direction. Stars indicate the western edge of the westward electrojet whose magnetic local time (MLT) is t_w.

We estimate Q_T (in watts) from

$$Q_i = \int_S \Sigma_P E^2 dS, \tag{31}$$

$$Q_A = 10^7 AE, \tag{32}$$

$$Q_{DR} = 4\times10^{13}(d\bar{D}st/dt + \bar{D}st/\tau) \tag{33}$$

where equation (32) is from *Ahn et al.* [1983]. The unit for *Dst* and *AE* is nanoteslas. The bar above *D* means "corrected for solar wind pressure." In (31), *S* is the area limited by $\Phi = 60°$, and τ is the characteristic ring current decay time. The value $\tau = 7$ hours will be used in the present study according to *Burton et al.* [1975a]. Despite the uncertainty in τ noted by *Zwickl et al.* [1987] due to the fast increase in Q_T at expansion phase onset, the timing obtained from the change of the sign of *P* is not correspondingly uncertain. A functional block diagram of the MIT-2 procedure is shown in Figure 4.

3. Timing of Typical Substorm Onsets and Phases

MIT-2-parameters are intended first of all, although not only, for substorm timing. This problem, addressed in this section, is important in itself and provides a test of the above described methods. We will describe concisely, as a typical example, the timing of the "average substorm." This timing method will also be used as a standard for performing the timing of the substorm on December 8, 1990, by comparison data observed with this standard. This period of study was chosen and the data originally gathered in support of the first Earth flyby of the Galileo spacecraft. However, we do not involve the Galileo data in this particular analysis.

Characteristics of the average substorm have been obtained from observations of 12 substorms using data of 80 and more ground-based magnetometers with geomagnetic latitude $\geq 40°$ [*Mishin et al.*, 1998]. Authors calculated the above listed MIT-2-parameters for all 12 events, but solar wind data were available for only 8 of them. The MIT-2 and all other parameters have been averaged by the method of superposed epochs separately over 12 and 8 substorms. Superposed tracks are given in Figure 5 where thick and thin lines mean averages over the 12 and 8 above mentioned events, respectively. Differences between the two lines are small and will be neglected. Figure 5 contains also the superposed X-magnetograms from ground-based magnetometers, which recorded substorm onsets in the sector of 21-01 hours MLT. Two superposed magnetograms are based on data from two regions, $\Phi = 55°$-$66°$ and $\Phi = 64°$-$72°$, with average geomagnetic latitudes of $\langle\Phi\rangle = 63.4°$ and $\langle\Phi\rangle = 68.3°$, respectively. Importantly, these two latitude zones are mapped to the near-Earth tail, where open flux reconnection has never been observed, and to the midtail, which is the most probable region of open tail reconnection during substorm. Two distinct onsets are clearly seen in the magnetograms.

Vertical lines mark these two onsets in all superposed tracks of Figure 5. One can see that the values of the *AE* index at the time of the two onsets are comparable, though the *AE* index is higher for the later one. In addition, the beginning of the later substorm intensification coincides in time with the start of the open flux

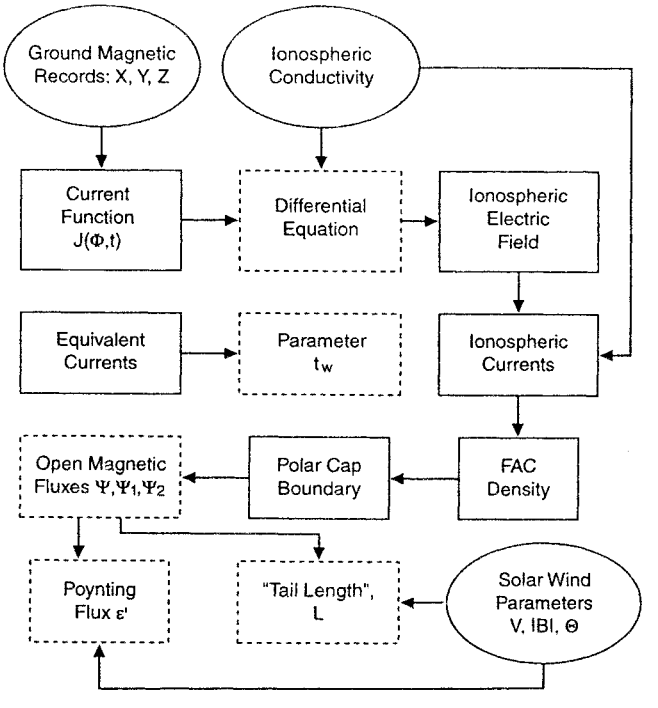

Figure 4. Functional block diagram of the MIT-2 method. FAC, field-aligned current.

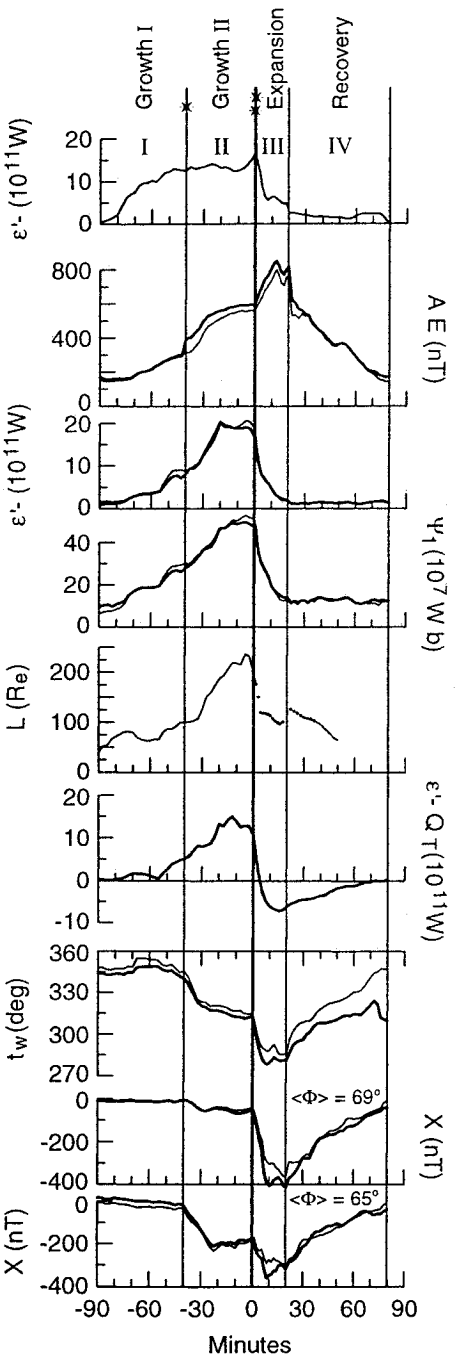

Figure 5. Superposed traces of the data from 12 substorms (thick lines) and from 8 substorms (thin lines). The abscissa is the substorm time, measured from the expansion onset. The borders of each phases are marked by the vertical lines. I, growth phase; II, first active phase; III, expansion phase; IV, recovery phase. The single star marks the start of the first active phase (and the first of special breakups). The double star denotes expansion onset.

(Ψ_1) decrease, which is the well-known signature of the expansion onset expected in the NENL model. Therefore the start time of the later onset is taken to be $t = 0$ for all superposed tracks in Figure 5.

We will first concentrate on the earlier onset. The plot of the parameter t_w in Figure 5 shows that this onset is accompanied by a weak decrease of t_w, which can be taken (see section 2.5) as a signature of small-scale current wedge formation and the cross-tail disruption. In the plot of the tail length L one can see that the earlier onset is accompanied by well-expressed tail stretching. Next, the plot of differences $\varepsilon' - Q_T$ demonstrates that this difference is positive during the earlier onset. This suggests that the power dissipated at this onset is supplied directly from the solar wind, without long storage in the magnetotail. On the whole, it is obvious that the earlier substorm onset is a driven disturbance, not associated with any signatures in Figure 5 of open tail reconnection. We will call the first type of onset the initial onset, as distinct from the later expansion onset.

In contrast to the earlier onset, the later one has all principal signatures of the expansion onset expected in the NENL model. One can see a fast and major decrease of L, i.e., the tail length contraction associated with the later onset. The plot of t_w shows a much stronger (than for the earlier onset) westward expansion of the westward electrojet, suggesting a stronger and wider current wedge, a large-scale cross-tail disruption, and magnetic field dipolarization. The difference ε'-Q_T changes its sign close in time to the later onset, from positive to negative, which implies unloading type of disturbance, when an intramagnetospheric energy source predominates. All these features taken together, and especially the rapid and deep decay of the open tail magnetic flux (see the plot of Ψ_1), are direct evidence of open tail reconnection, which begins simultaneously with the later onset.

Thus the data in Figure 5 imply that two types of substorm onsets exist in an average substorm, which are created without and with open tail reconnection, respectively. If this is the case, a typical substorm consists of four phases, whose definitions are the following (see Figure 5). The first two of our phases constitute what is usually called the growth phase [*McPherron*, 1970]; the second two are the expansion and recovery phases.

1. The driven phase is characterized by growth of the open magnetic flux Ψ_1, the tail length L, and the energy flux to the magnetosphere from the solar wind (ε') not accompanied by a fast enhancement of activity or by substorm onset. The difference ε'-Q_T has a positive sign, and the parameter t_w is ~ 340°, corresponding to a DP2 type of an equivalent current system. This phase begins when the Perreault-Akasofu index ε begins to grow.

2. The loading phase (first active phase) is characterized by continuing growth of Ψ_1, L, and ε' as expected in the growth phase, and the difference $\varepsilon' - Q_T$ remains positive, but there arises a fast onset of the auroral electrojet perhaps associated with the significant change in the rate of convection (see t = -35 min in the X-magnetogram for <Φ> ~ 64°). Values of t_w decrease, indicating an initial stage of transition from DP2 to DP1 behavior and small-scale current wedge formation. However, taken together, these data do not contain sufficient signatures of open tail reconnection.

3. The expansion phase (second active phase) is characterized by a fast decline of Ψ_1, L, and ε', with the activity level remaining the same or (more often) increasing. This later onset begins as an expansion onset. The difference $\varepsilon' - Q_T$ changes its sign. The value of t_w is close to 18 hours MLT, which is the signature of a DP1 type of an equivalent current system and of a full-scale current wedge formation together with a much stronger near-tail magnetic field dipolarization. These data, all together, are the necessary and sufficient signature of open tail reconnection.

4. The recovery phase is the recovery of the magnetosphere to its initial state.

In section 4, this scenario will be used as a standard against which to study the December 8, 1990, events, in order to test and develop it on data from a chain of weak, overlapping, winter substorms.

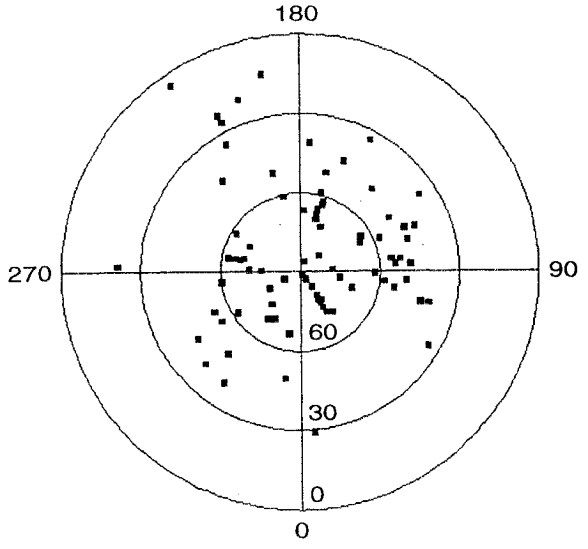

Figure 6. Magnetic observatory locations used in this study expressed in geomagnetic coordinates Φ, Λ.

4. Database and Results of the Selected Events Study

Information to be used in the study of the December 8, 1990, events consists of plots of solar wind parameters measured aboard IMP 8, plots of *AE* and *Dst* indices, and plots of the MIT-2 parameters. We calculate *AE* indices in the usual way using the magnetograms from 28 stations between 60° and 77° in latitude. *Dst* indices were prepared by T. Kamei (Kyoto University) and M. Sugiura (Tokai University). Use will also be made of magnetograms from high-latitude magnetic stations to enable timing and spatial localization of local magnetic substorm onsets.

In calculating the MIT parameters, measurements of geomagnetic variations at 81 ground-based magnetometers at geomagnetic latitudes from 0° to 90° were used (see Figure 6). The reference level of variations is the average level in the interval 1200-1230 UT, December 8, 1990, with the parameters: $AE = 90$ nT, $Dst = -6$ nT, $V_{SW} = 365$ km s^{-1}, and $n = 5.2$ cm^{-3}.

Solar wind parameters are shown in Figure 7, as well as plots of *AE* and *Dst* indices. Figure 8 shows plots of the variation of Perreault-Akasofu's ε and the above listed MIT-2-parameters calculated with 5-min steps or, sometimes, 1-min steps. Plots of the polar cap electric potential drop U_{pc} and the intensity of the westward (I_w), and eastward (I_e) auroral electrojets are also shown in Figure 8. (These three parameters play only an auxiliary role in this study; for the method of their calculation, see *Mishin et al.* [1997].) Figure 9 presents magnetograms from those ground-based magnetic stations which "saw" substorm onsets.

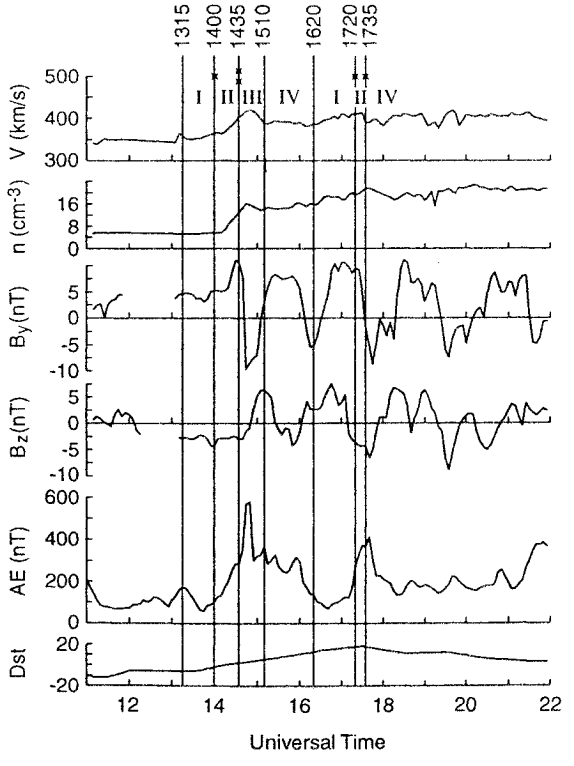

Figure 7. Solar wind parameters at the nose of the magnetopause and AE and Dst indices for the interval 1100-2200 UT, December 8, 1990. Phase IV is the recovery phase. The other designations are the same as those in Figure 5.

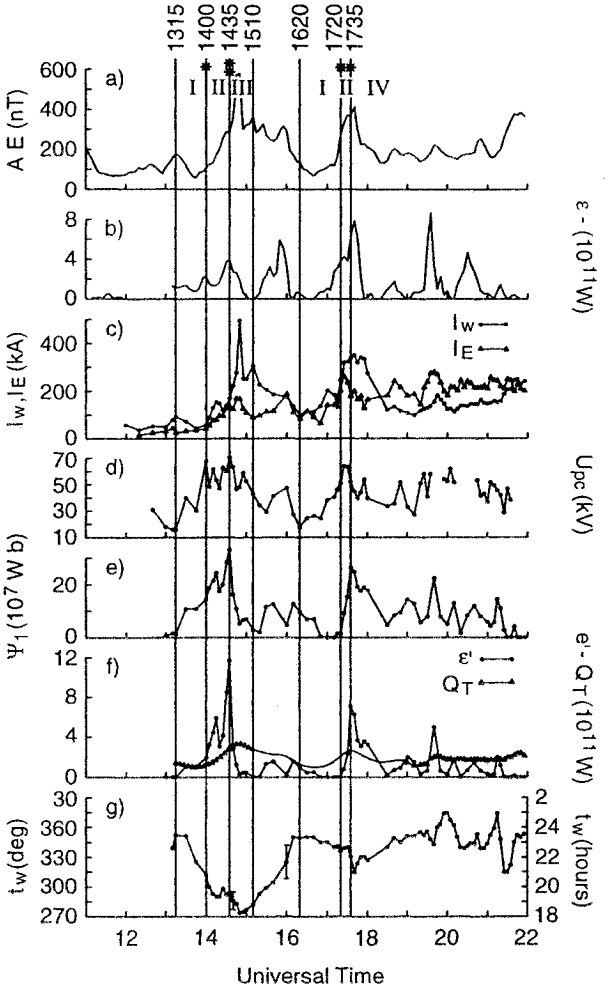

Figure 8. (a) AE indices. (b) Perreault-Akasofu's parameter ε. (c) Westward electrojet intensity IW and eastward electrojet intensity IE. (d) Polar cap potential Upc. (e) Open magnetic flux Ψ1. (f) Poynting vector flux ε′ and total substorm power QT. (g) Index tW, which is the MLT of the western edge of the westward electrojet. The other designations are the same as those in Figure 5.

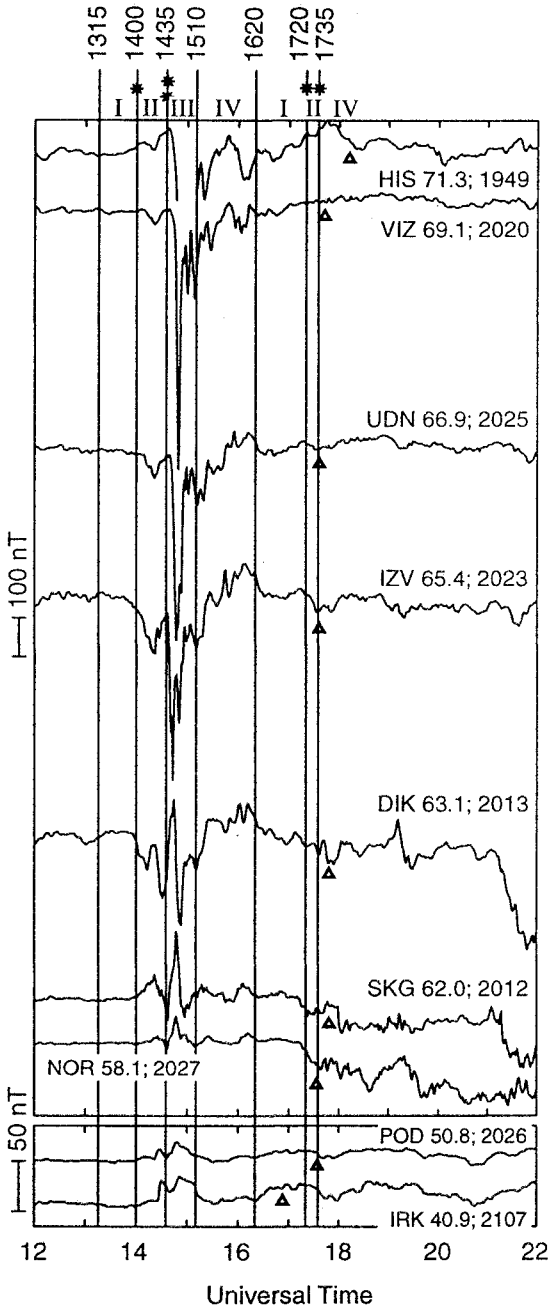

Figure 9. The X component magnetograms from the ground-based stations close to 2030 MLT. Shown are geomagnetic latitudes and local geomagnetic time (MLT) for 1400 UT. Triangles mark midnight (0000 MLT). The other designations are the same as those in Figure 5. HIS, Heiss Island; VIZ, Vize; VDN, Uedineniya; IZV, Izvestiya; DIK, Dixon Island; SKG, Sopochnaya; POD, P. Tunguska; IRK, Irkutsk; NOR, Norilsk.

At the time of interest the GSM x, y, and z average coordinates of IMP 8 were 38.4, 4.2, and -2.3 R_E, respectively. A delay of 10 min was calculated in the usual way to take into account the path of the solar wind from IMP 8 to the nose of the magnetopause. Thus the solar wind parameters and values of ε and L are drawn in Figures 7, 8, and 10 with a delay of 10 min. The event of our interest, in the interval 1000-2200 UT, December 8, 1990, is the chain of weak disturbances with $AE_{max} < 600$ nT and characteristic values of $\langle AE \rangle \leq 300$ nT.

While being biased to the substorm scenario presented in section 3, we marked off the instants shown in Figures 8-11 by vertical lines. Each of these lines designates the start of one of the substorm phases. The time of the start and end of these phases is indicated to an accuracy of ~5 min.

IMF data were unavailable for the interval ~1209-1309 UT. Therefore we begin our study of the first substorm interval at 1315 UT, although the substorm itself began earlier.

The interval 1315-1400 UT belongs to the growth phase of the first substorm because in this interval no signatures of substorm onsets are observed, but at 1315 UT a growth of Ψ_1 and the polar cap potential drop U_{pc} begins (see Figure 8). The value of Ψ_1 increases in the course of the inferred growth phase by 4×10^8 W, and the value of U_{pc} increases by more than a factor of 2 and reaches >60 kV. Values of t_w are preserved at a level > 315°, which corresponds to the initial stage of a DP2 to DP1 transition.

The time 1400 UT coincides with the substorm onset which is seen in X-magnetograms from ground-based magnetometers at geomagnetic latitudes 60°-68° in the sector 2000-0200 MLT (Figures 9 and 10). This means that the new regime has just begun. As seen in Figure 7, growth of Ψ_1 and ε' continues following the above mentioned onset of a new regime. The value of the parameter t_w has decreased in the course of the new regime, thus indicating the continuation of the transition DP2 to DP1 but only to a level >285°; that is, the transition had not yet been completed. These signatures correspond to the beginning of the first active phase, without open tail reconnection. Hence the 1400 UT onset

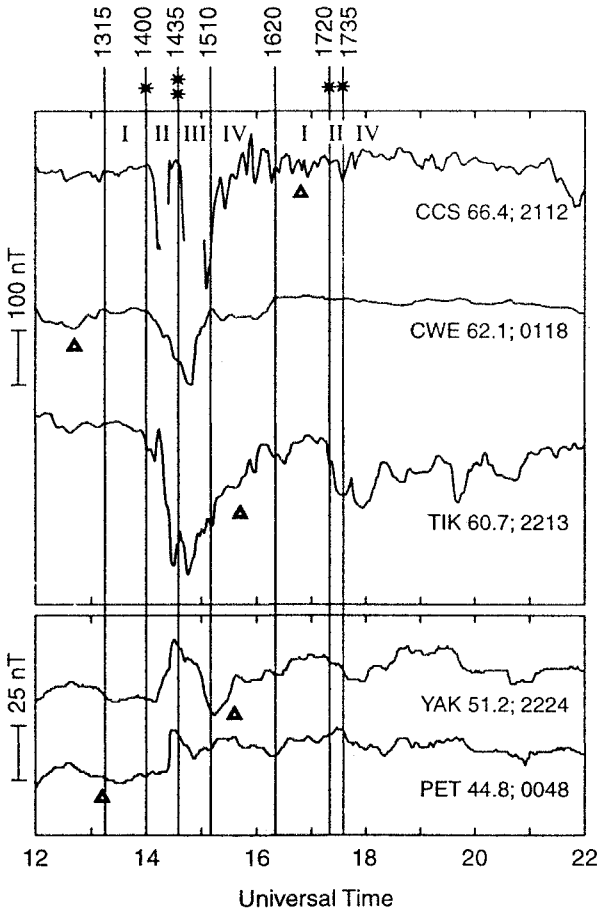

Figure 10. The X component magnetograms on meridians close to 2300 MLT. CCS, Cape Chelyuskin; CWE, Cape Wellen; TIK, Tixie Bay; YAK, Yakutsk; PET, Petropavlovsk.

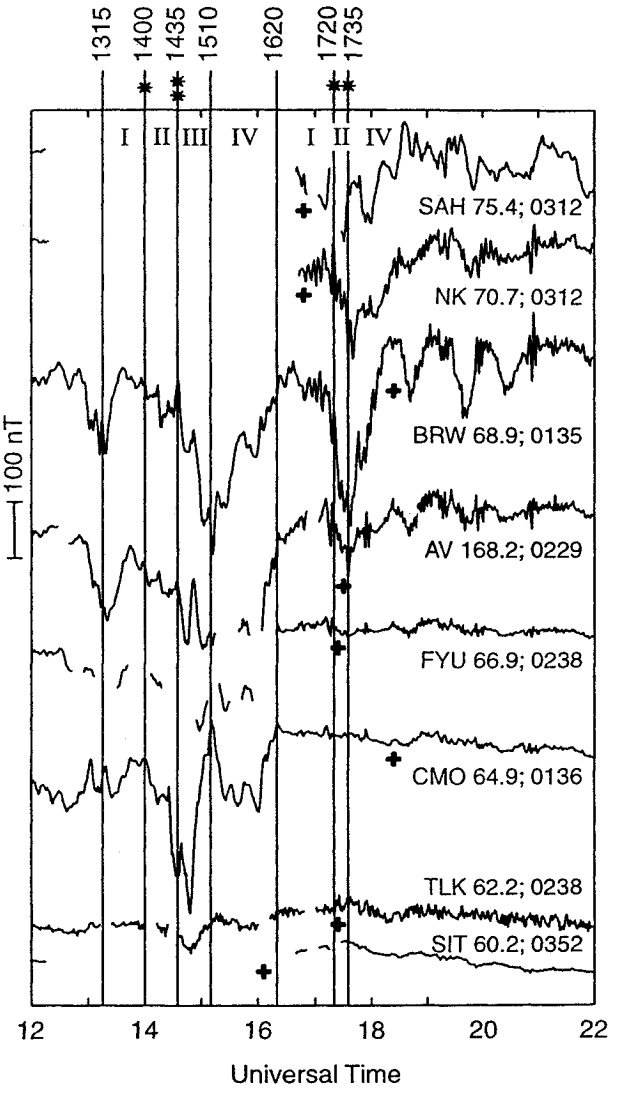

Figure 11. The X component magnetograms on meridians close to 0200 UT. Pluses mark 0600 MLT. SAH, Sach's Harbor; INK, Inuvik; BRW, Barrow Arctic Village; FYU, Fort Yukon; CMO, College; TLK, Talkeetna; SIT, Sitka.

was the initial onset not the expansion onset. Note further that in the interval 1400-1435 UT the inequality $\varepsilon' > Q_T$ holds, which also corresponds to the predominance of the external source of the observed disturbance power and hence to the expected signature of the first active phase.

At 1435 UT *a* next, stronger substorm onset begins (Figures 9 and 10). It differs from the preceding one primarily in that it coincides with the beginning of a rapid drop of Ψ_1, which is the necessary signature of open tail reconnection. At 1435 UT there is also a rapid drop of t_w to a level ~270° characteristic of the DP1 type of the equivalent current system. The DP1 type is the signature of large-scale, cross-tail current disruption. One more substantial feature is the fact that the 1435 UT onset was observed by ground magnetometers at higher latitudes than the preceding one (see Figure 8). Further, at ~1435 UT there occurs a sudden acceleration in the growth of the *AE* index whose value has become twice as large during the 15 min after 1435 UT. At the same time, the intensity of the westward electrojet also becomes more than twice as large. Lastly, we note that in the interval 1440-1500 UT the inequality $\varepsilon' < Q_T$ holds, which corresponds to the predominance of the intramagnetospheric source of the observed disturbance power and to the expected signature of the (unloading) second active phase. On the whole, we conclude that at 1435 UT there was a series of the expected signatures of a sudden onset of open tail reconnection; that is, the 1435 UT onset is the expansion onset.

The time 1510 UT is marked in Figures 7-11 as the beginning of the fourth phase of the first substorm. The main characteristics of this phase, seen in Figure 8, are a low (background) level of Ψ_1 and ε', a drop to the background level of values of *AE* and I_w; and the return of t_w to values corresponding to the DP2 type of the equivalent current system. Thus the fourth phase at 1510-1620 UT contains all the signatures of a recovery phase expected from ground observations. However, it was a recovery with traces of the magnetospheric response to the impulse of ε growth seen in Figure 8 in the interval 1510-1620 UT. Because of this impulse, the fast decline of the *AE* indices was stopped at a level of ~300 nT for ~40 min. We will refer to the interval 1510-1620 UT as the recovery phase, although we will keep in mind the above mentioned superposed impulse of ε growth.

On the whole, the substorm under consideration, in the time interval 1315-1620 UT, contains all four phases of a typical substorm, providing support for the "substorm with two active phases" scenario (section 3). A special feature is the impulse of growth of the Perreault-Akasofu index ε in the interval 1500-1600 UT. The impulse was relatively long lasting, and the peak value of this purported solar wind Poynting vector flux (~6×10^{11} W) was close to the largest value for the entire interval 1200-2200 UT being considered. This impulse caused only a small increase in the calculated magnetotail Poynting vector ε', but perhaps just this was sufficient to sustain the observed activity on the level ~300 nT for ~40 min. This lack of a quantitative correlation between solar wind and tail Poynting fluxes is consistent with our discussion of the source of the tail Poynting flux in section 2.3.

At ~1620UT, a next impulse of growth of the Perreault-Akasofu index ε started. The impulse was of a duration of > 1 hour, and its peak value was 8×10^{11}W. The observed peak value of ε' reached ~5×10^{11} W. Thus this impulse of growth of ε, in contrast to the previous case, created a corresponding growth of the calculated tail Poynting flux ε', although the ratio ε'/ε was markedly less compared with that in the interval 1400-1510 UT.

The beginning of the magnetospheric response to ε' growth is seen in Figure 8 in the interval 1620-1720 UT as a slow growth in intensity of the westward and eastward auroral electrojets and a corresponding growth of *AE* index to ~300 nT. In this interval a growth of U_{pc} and a slow drop of t_w also take place, indicating a weak enhancement of tail current disruption. Substorm onsets were not observed in the above interval (Figures 9-11). All the aforesaid corresponds to the identification of the interval 1618-1720 UT as the prephase of the second substorm. An important peculiarity of this part of the growth phase of the second substorm is the fact that the value of L did not increase during this phase, while in the first substorm the value of L ~250 R_E was reached (Figure 10).

In the interval 1720-1735 UT the above mentioned tendencies remained. Values of the *AE* index, eastward and westward electrojet intensities, and U_{pc} reached maximum values of ~400 nT, 350 nT and >60 kV, respectively; the value of t_w continued to grow. Note that the growth of Ψ_1 and the observed Poynting flux ε' were not registered during the above growth phase, but they started at ~ 1720 UT, and a value of ε' ~5×10^{11} W was reached

(Figure 8). Near the beginning of the interval considered, on the X-magnetogram from Tixie (Φ = 60.5°, premidnight sector), one can see a rapid beginning of a negative bay (Figure 10). Similar signatures, together with trains of Pc5 pulsations, are evident on magnetograms from Canadian stations Inuvik, Barrow, and Arctic Village (Figure 11). These are signatures of the loading onset. Thus we identify the interval 1720-1735 UT as the part of the first active phase, although the observed onset was relatively weak and was narrowly localized in space.

The time 1735 UT is marked in Figures 7-11 as the beginning of a rapid drop of Ψ_1, ε', and t_w, which corresponds to the necessary signatures of an expansion onset. However, these signatures were not sufficient. The transition from DP2 to DP1 currents terminated at its initial stage (at t_w >315°). Plots of the *AE* index and I_w did not show any growth of activity. In Figure 10, near 1735 UT, one can detect only a slight trace of the substorm onset localized near Tixie Bay. The subsequent, longer than 1-hour interval showed a decline of activity and the recovery of the equivalent current system to the DP2 type (see the plot of t_w). Thus the above noted necessary conditions of an expansion onset were not realized. Therefore we finally identify the events in the interval 1720-1740 UT as the first active phase of the second substorm. Further, in the interval ~1740-1830 UT a decay of activity and a decrease of the Ψ_1, ε' values, and also the return from DP2 to DP1 are seen in Figure 8, which are sufficient signatures of the recovery phase. On the whole, the interval 1620-1830 UT included three first phases of a typical substorm which were not accompanied by the expansion phase.

In the subsequent interval (1830-2200 UT), the activity remained at the level of *AE*~200 nT. Figure 8 shows that the activity level was sustained by a chain of impulses of growth in energy flux to the magnetosphere (ε). Peak values of ε were in excess of 1×10^{11} watt, and around 1900 UT a value of $\varepsilon\sim8\times10^{11}$ W was attained. However, these impulses of the anticipated Poynting flux ε did not produce any appreciable growth of the observed Poynting flux to the magnetosphere (ε'). Values of ε' remained near a threshold level of 1×10^{11} W. On the whole, the 2-hour interval (1830-2200 UT) was observed as a continuation of the preceding 2-hour interval with loading onsets.

5. Discussion and Conclusions

In section 4 we performed timing studies of the December 8, 1990, events using MIT-2 parameters and the corresponding substorm scenario as essential additional tools. In particular, we assumed that a sharp decrease of Ψ_1 value, accompanied by corresponding changes of tail length L and the power difference $\varepsilon' - Q_T$, as well as by a growth of the activity level, is the necessary and sufficient signature of open flux reconnection, in contrast to the period of Ψ_1 growth. In this connection, two possible concerns about our approach should be addressed. First, it might be thought that the four parameters, Ψ_1, ε', L, and $\varepsilon' - Q_T$, are not absolutely independent but are interrelated. Second, one might object to our interpretation of the expansion phase onset as the secession of storage since open flux reconnection can occur even during a period of open flux increase if open flux is added more quickly by dayside reconnection than it is removed from the nightside by tail reconnection. These concerns could cast doubt on the principal conclusions of our substorm timing study, according to which there are two types of substorm onsets and correspondingly two active phase without and with open flux reconnection in the tail, respectively.

With regard to the first concern, we note, as a counterargument, that the above mentioned four parameters essentially complement one another. For example, a sharp decrease of the value of Ψ_1 can not be taken as the signature of open flux reconnection if it is not accompanied by the strictly specified changes of the above mentioned other parameters: (1) L should be decreasing too, together with Ψ_1, although it is seen from (20) that if there is no open flux reconnection, the value of L should not change or should even increase when the M value decreases (that is most often observed as the primary cause of expansion onset), because Ψ_1 would decrease following M but not faster than M in (17); (2) The difference $\varepsilon' - Q_T$ should become negative simultaneously with the onset of the Ψ_1 decrease, although a positive sign is typical of the growth phase of Ψ_1 (Figure 5), and it would be difficult to understand why it should become negative suddenly without open flux reconnection.

Another response is that for substorm timing we use not only the four above mentioned parameters but essentially more information, obtained independently of Ψ_1, including parameters t_w, Q_T, ground-based magnetograms in two different latitude zones, as well as *AE* indices, the ε index, data of ISEE 3 and IMP 8, and other traditionally used data. This information supports the results of substorm timing based on the MIT-2-parameters. Moreover, we have seen that ground-based magnetograms in two neighboring high-latitude zones give immediate evidence that two types of substorm onsets are typically observed, without and with open flux reconnection, respectively.

With regard to the second concern, this situation can and does occur. However, even if open flux reconnection develops in the course of the loading phase (that is, when Ψ_1 and activity both increase), this process by definition cannot be predominant. The relative lengths of the growth and expansion phases demonstrate that for substorms the tail reconnection rate exceeds the dayside reconnection rate. When the dayside reconnection rate exceeds or equals that in the tail, then we expect that a storm will ensue. However, in substorms in which we clearly have a sequence of different states in the tail, it is sufficient to conclude that two physically different processes, i.e., without and with open flux reconnection, are the predominant ones in the first and second active phases, respectively. Moreover, onsets of the first and second type do not comprise and do comprise sufficient signs of open flux reconnection, respectively.

Now we can go back to the December 8, 1990, events. The entire interval considered was separated into three substorm-like intervals, namely, 1315-1620, 1620-1830, and 1830-2200 UT. The first interval contains all four typical phases of a typical ("average") substorm, providing support for the "substorm with the two active phases scenario" in section 3. The second interval (1620-1830 UT) included only two first phases of a typical substorm and the initial stage of the recovery; that is, it did not involve an expansion phase. The last interval (1830-2200 UT) contained two impulses with high peak values of the Perreault-Akasofu indices ε but without an adequate response in *AE* indices, that is, it was an interval of loading onsets or the regime of the first active phase.

During the entire interval (1315-2200 UT) under study, five impulses of growth of the Perreault-Akasofu indices ε took place, which have comparable peak values of ε and values of $\int\varepsilon' dt$ (see Figure 8). However, the index ε is a proxy for the energy that we expect to be entering the combined magnetosphere-ionosphere system compared to ε' that is an approximation of the energy that is being stored in the tail itself (see section 2). The ratio ε'/ε was very different for the neighboring ε impulses, and only one im-

pulse of ε (at 1315-1510 UT) was accompanied by a normal magnetospheric response, i.e., the substorm with the signatures of the expansion onset. Why? This variability should not be surprising since the Poynting flux in the tail does not derive directly from the Poynting flux in the solar wind.

Compare the integral energy input $W = \int \varepsilon' dt$ during the growth phase of each substorm on December 8, 1990, with that expected for a typical substorm with a clearly expressed expansion onset. For the CDAW6 substorm, 1054 UT, March 22, 1979, the appropriate estimates were obtained with independent methods [*Baker et al.*, 1983; *Mishin*, 1991, and references therein]. For the CDAW9C1 substorm on May 3, 1986, the corresponding estimates have been obtained, also by independent methods [*Baker et al.*, 1997; *Mishin et al.*, 1996]. Both these CDAW events were strong substorms. Four estimates of W for these substorms lie within values $3\text{-}5\times10^{15}$ J. Thus, for the weak substorms on December 8, 1990, we would expect values $W\approx1\times10^{15}$ J or more. Such a threshold value of accumulated energy (W) was reached in the course of the loading phases of the 1315-1620 UT substorm. Indeed, from the data in Figure 8 we find

$$W = \int_{1315UT}^{1435UT} \varepsilon' dt = 2\times10^{15} J$$

For all subsequent impulses of growth of ε′, from the data in Figure 8 we have values of $W<1\times10^{15}$ J. This is true even for the interval 1700-1800 UT, where ε′ reached a value of $\sim5\times10^{11}$ W, but the duration of the loading phase was only 15 min. Thus the stored energy W during the loading phase was essentially a different quantity for each substorm.

Turning this problem around we can calculate the effectiveness of the "Poynting flux" parameter ε in predicting solar wind energy input to the tail. Taking the ratio $\kappa = \varepsilon'/\varepsilon$ to be the effectiveness of solar wind energy transfer to the magnetosphere, we obtain the plot of variation of the effectiveness κ shown in Figure 12. Figure 12 also presents a plot of the variation of "the tail length" L obtained by assuming $\kappa = (L/L_0)^2$, where $L_0 = 130\ R_E$ (see section 2). In the adopted model the observed variability of the effectiveness of energy transfer is explained by variations of the calculated L parameter. The main question is, How reliable are these calculated values? Of course, they are only approximate values, but the supporting arguments are the following. First, an abrupt decrease of the calculated value of L around 1435 UT (Figure 12) corresponds to an independently made identification of this instant of time as the expansion onset, i.e., the beginning of open tail reconnection and the abrupt contraction of the tail length. Second, the increase of the L-calculated value by a factor of ~2 in the course of the loading phases of the "complete" substorm, i.e., at 1315-1435 UT, does correspond, qualitatively at least, to results expected from earlier studies [*Schindler et al.*, 1989; *Cowley*, 1992]. Third, the calculated low value of L for the interval 1510-1620 UT explains why only a loading onset but not a full expansion onset was observed at this time and has by itself a simple and natural interpretation. Indeed, at ~1435 UT the low value of L was established by open tail reconnection. The following impulse of ε growth (at ~1510-1620 UT) would sustain this process and, as a result, would keep the low value of L until ~1700 UT, when the new impulse of ε growth occurred (Figure 12). This new impulse would maintain the continuation of open tail reconnection, which would prevent the storage of energy and explain the fact that at ~1735 UT the expansion onset was not observed in spite of the fact that the principal necessary conditions for it (the fast and deep drop of Ψ_1) were satisfied.

Thus we interpret the occurrence of a loading onset or an expansion onset to depend on the stored free energy W, controlled by the tail length L, which itself is controlled by ε′. A similar role for the free energy stored in the magnetotail was also suggested by *Koskinen et al.* [1993]; *Ohtani et al.* [1993]; and *Nakamura et al.* [1994]. Ohtani et al. supposed also that the ionospheric conductivity determines whether expansion onset or pseudobreakup will take place. This supposition is not supported by our results, although the conductivity perhaps plays an important role for the creation of the first of multiple loading onsets. Our variant of this interpretation is in some sense intermediate between those of Koskinen-Nakamura and Ohtani.

We used the substorm scenario where the tail length L and the effectiveness κ both grow concurrently during the loading phase until some critical levels are attained, which switch on the expansion onset with open flux reconnection. This is a scenario similar to that "with two active phases and the tail-stretching feedback." In this scenario (see *Mishin et al.* [1997] for more detail) the first active phase of a typical substorm is the phase of loading onsets produced by instabilities in the innermost current sheet, which do not involve the open tail reconnection but do involve a chain of processes created by the tail stretching with positive feedback between the solar wind–magnetosphere dynamo and the magnetosphere itself. The ionosphere does not play a crucial role in the transition from the regime of loading onsets to the expansion phase, although it can influence the intensity of the loading onset itself. The main peculiarities of the tail-stretching-feedback scenario in comparison with other models is the tail-stretching feed-

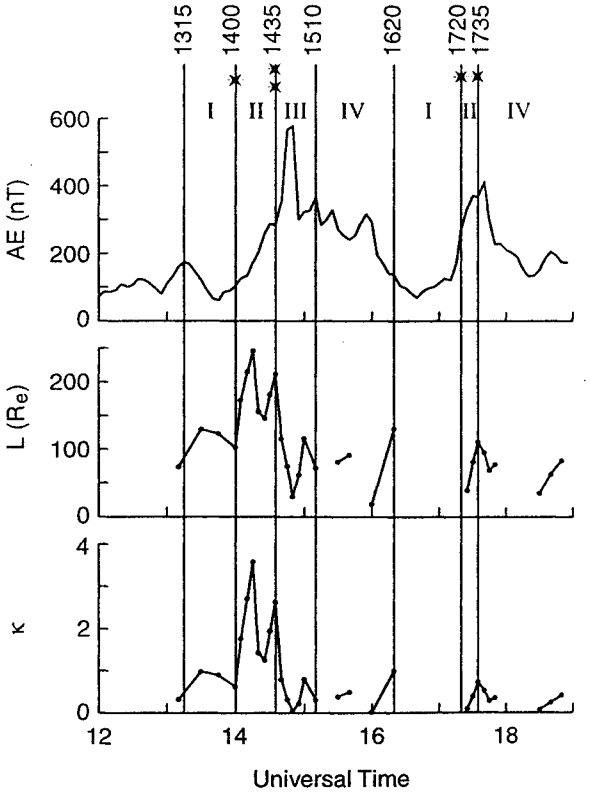

Figure 12. AE indices, the magnetospheric tail length L, and the effectiveness of the solar wind energy transfer to the magnetosphere (κ). Double and single stars are the initial and expansion substorm onsets, respectively.

back itself, which organizes successive phases of a typical substorm, including two active phases (and two corresponding types of the substorm onsets) without and with open flux reconnection, respectively.

To recapitulate, this work shows that the timing of substorms and the understanding of their principal physical components can be improved, if the above mentioned MIT-2-parameters are used in addition to the traditional tools, as well as definitions of substorm phases and the two types of onsets expressed in terms of MIT-2 parameters. This was shown, however, only by a specific example. There are many outstanding questions. For example, our model does not explain the low level of the effectiveness κ and the parameter L during the interval from 1800 to 2200 UT. This question remains open as well as the question of the numerical accuracy of ε', L, and W estimates obtained by the method of section 2. On the one hand, such estimates obtained in the present paper do not contradict those that are available from the literature. On the other hand, MIT-2 estimates are only indirect estimates, direct methods to estimate the above listed parameters do not exist, and the existing, indirect methods give us only fragmentary and crude estimates. Taking into account these circumstances and the great diversity of substorm forms, it is clear that many more theoretical and observational studies are required to solve the remaining outstanding questions.

Acknowledgments. Partial funding was provided by RFFR, grants 96-05-64348, 98-05-65406, and 99-05-65234. Work at UCLA was supported by the National Science Foundation under research grant ATM 98-03441.

Michel Blanc thanks both referees for their assistance in evaluating this paper.

References

Ahn, B.-H., R. M. Robinson, Y. Kamide and S.-I. Akasofu, Electric conductivities, electric fields and auroral particle energy injection rate in auroral ionosphere and their empirical relation to the horizontal magnetic disturbances, *Planet. Space Sci., 31,* 641-653, 1983.

Akasofu, S.-I., *Physics of Magnetospheric Substorms,* 599 pp., D. Reidel, Norwell, Mass., 1977.

Akasofu, S.-I., Energy coupling between the solar wind and magnetosphere, *Space Sci. Rev., 28,* 121-190, 1981.

Baker, D. N., R. D. Zwickl, S. J. Bame, and E. W. Hones Jr., An ISEE 3 high time resolution study of interplanetary parameter correlations with magnetospheric activity, *J. Geophys. Res., 88,* 6230-6242, 1983.

Baker, D. N., T. I. Pulkkinen, R. L. McPherron, and C. R. Clauer, Multi spacecraft study of a substorm growth and expansion phase features using a time-evolving field model, in *Solar System Plasmas in Space and Time, Geophys. Monogr. Ser., vol. 84,* edited by J. L. Burch and J. H. Waite Jr., pp. 101-110, AGU, Washington, D.C., 1994.

Baker, D. N., T. J. Pulkkinen, V. Angelopoulos, W. Baumjohann, and R. L. McPherron, Neutral line model of substorms: Past results and present view, *J. Geophys. Res., 101,* 12,975-13,010, 1996.

Baker, D. N., T. I. Pulkkinen, M. Hesse, and R. L. McPherron, A quantitative assessment of energy storage and release in the Earth's magnetotail, *J. Geophys. Res., 102,* 7159-7168, 1997.

Birn, J., E. W. Hones Jr., J. D. Craven, L. A. Frank, R. D. Elphinstone, and D. P. Stern, On open and closed field line regions in Tsyganenko's field model and their possible associations with horse collar auroras, *J. Geophys. Res., 96,* 3811-3817, 1991.

Birn, J., M. Hesse, and K. Schindler, MHD simulations of magnetotail dynamics, *J. Geophys. Res., 101,* 12,939-12,954, 1996.

Burton, R. K., R. L. McPherron and C. T. Russell, An empirical relationship between interplanetary conditions and *Dst, J. Geophys. Res., 80,* 4204-4214, 1975a.

Burton, R. K. et al., The terrestrial magnetosphere: A half-wave rectifier of the interplanetary electric field, *Science, 189,* 717-718, 1975b.

Chapman, S., and J. Bartels, *Geomagnetism,* 1049 pp., Oxford Univ. Press. New York, 1940.

Cowley, S. W. H., The role and location of magnetic reconnection in the geomagnetic tail during substorms, in *Substorms 1: Proc. First International Conference on Substorms, Eur. Space Agency Spec. Publ., ESA SP-335,* 401-404, 1992.

Dungey, J. W., Interplanetary magnetic field and the auroral zones, *Phys. Rev. Lett., 6,* 47-48, 1961.

Elphinstone, R. D., D. Hearn, J. S. Murphree, and L. L. Cogger, Mapping using the Tsyganenko long magnetospheric model and its relationship to Viking auroral images, *J. Geophys. Res., 96,* 1467-1480, 1991.

Erickson, G. M., W. J. Burke, M. Heinemann, J. S. Samson, and N. Maynard, Towards a complete conceptual model of substorm onsets and expansions, in *Proceedings of the International Conference on Substorms 3 ICS-3, Eur. Space Agency Spec. Publ., ESA SP 389,* 423-428, 1996.

Fukushima, N., Generalized theorem for no ground magnetic effect of vertical current connected with Pedersen current in the uniform or the conductivity ionosphere, *Rep. Ionos. Space Res. Jpn., 30,* 35-40, 1976.

Holzer, R. E., R. L. McPherron, and D. A. Hardy, A quantitative empirical model of the magnetospheric flux transfer process, *J. Geophys. Res., 91,* 3287-3293, 1986.

Kamide, Y., and A. D. Richmond, Ionospheric conductivity dependence of electric fields and currents estimated from ground magnetic observations, *J. Geophys. Res., 87,* 8331-8337, 1982.

Kamide, Y., A. D. Richmond, and S. Matsushita, Estimation of ionospheric electric fields, ionospheric currents, and field-aligned currents from ground magnetic records, *J. Geophys. Res., 86,* 801-813, 1981.

Kan, J. R., A global magnetosphere-ionosphere coupling model of substorms, *J. Geophys. Res., 98,* 17,263-17,275, 1993.

Kan, J. R., and L. C. Lee, Energy coupling function and solar wind: Magnetosphere dynamo, *Geophys. Res. Lett., 6,* 577-580, 1979.

Koskinen, H. E. J., R. E. Lopez, R. J. Pellinen, T. I. Pulkkinen, D. N. Baker, and T. Bosinger, Pseudobreakup and substorm growth phase in the ionosphere and magnetosphere, *J. Geophys. Res., 98,* 5801-5813, 1993.

Lui, A. T. Y., A synthesis of magnetospheric substorm models, *J. Geophys. Res., 96,* 1849-1856, 1991.

Lui, A. T. Y., Current disruption in the Earth's magnetosphere: Observations and models, *J. Geophys. Res., 101,* 13,067-13,088, 1996.

Maynard, N. C., W. G. Burke, G. M. Erickson, E. M. Babinska, and A. G. Yahnin, Magnetosphere-ionosphere coupling during substorm onset, in *Proceedings of the International Conference on Substorms 3, Eur. Space Agency Spec. Publ., ESA SP 389,* 301-305, 1996.

McPherron, R. L., Growth phase of magnetospheric substorms, *J. Geophys. Res., 75,* 5592-5599, 1970.

McPherron, R. L., C. T. Russell, and M. Aubry, Satellite studies of magnetospheric substorms on August 15, 1978, 9, Phenomenological model for substorms, *J. Geophys. Res., 78,* 3131-3149, 1973.

Mishin, V. M., On the electric currents in the magnetosphere, *Geomagn. Aeron., 8,* 168-171, 1968.

Mishin, V. M., The magnetogram inversion technique and some applications, *Space Sci. Rev., 53,* 83-163, 1990.

Mishin, V. M., The magnetogram inversion technique: Applications to the problem of magnetospheric substorms, *Space Sci. Rev., 57,* 237-337, 1991.

Mishin, V. M., A. D. Bazarzhapov, and G. B. Shpynev, Electric fields and currents in the Earth's magnetosphere, in *Dynamics of the Magnetosphere, Astrophys. Space Sci. Libr., vol. 78,* edited by S.-I. Akasofu, pp. 249-268, D. Reidel, Norwell, Mass., 1980.

Mishin, V. M., S. B. Lunyushkin, D. S. Shirapov, and W. Baumjohann, Model of the ionospheric conductivity spatial distribution, (in Russian) in *Res. on Geomagn. Aeron. Sol. Phys., 63,* 108-115, 1983

Mishin, V. M., S. B. Lunyushkin, D. S. Shirapov, and W. Baumjohann, A new method for generating instantaneous ionospheric conductivity models using ground-based magnetic data, *Planet. Space Sci., 34,* 713-722, 1986.

Mishin, V. M., A. D. Bazarzhapov, T. I. Saifudinova, S. B. Lunyushkin, D. S. Shirapov, J. Woch, L. Eliasson, H. Opgenoorth, and J. S. Murphree, Different method to determine the polar cap area, *J. Geomagn. Geoelectr., 44,* 1207-1214, 1992.

Mishin, V. M., A. D. Bazarzhapov, T. I. Saifudinova, S. B. Lunyushkin, Investigation of the CDAW9C-1 substorm, in *Proceedings of International Conference on Substorms 3, Eur. Space Agency Spec. Publ., ESA SP 389,* 121-125, 1996.

Mishin, V. M. et al., A study of the CDAW 9C substorm of May 3, 1986, using magnetogram inversion technique 2, and a substorm scenario with two active phases, *J. Geophys. Res., 102,* 19,845-19,859, 1997.

Mishin, V. M., T. I. Saifudinova, A. D. Bazarzhapov, L. P. Block, and H.

Opgenoorth, Existing methods of substorm timing neglect the two-stage development of a typical substorm active phase, in *Substorms-: International Conference on Substorms 4,* edited by S. Kokubun and Y. Kamide, pp. 87-90, Terra Sci., Tokyo, 1998.

Nakamura, R. D., D. N. Baker, R. D. Belian, and E. A. Bering, Particle and field signatures during the pseudobreakup and major expansion onset of substorms, *J. Geophys. Res., 99,* 207-221, 1994.

Ohtani, S. et al., A multisatellite study of a pseudo-substorm onset in the near-Earth magnetotail, *J. Geophys. Res., 98,* 19,355-19,367, 1993.

Perreault, P., and S.-I. Akasofu, A study of geomagnetic storms, *Geophys. J. R. Astron. Soc., 54,* 547-573, 1978.

Petrinec, S. M., and C. T. Russell, Near-Earth magnetotail shape and size as determined from the magnetopause flaring angle, *J. Geophys. Res., 101,* 137-152, 1996.

Pulkkinen, T. I. et al., Two substorm intensifications compared: Onset, expansion, and global consequences, *J. Geophys. Res., 103,* 15-27, 1998a.

Pulkkinen, T. I., D. N. Baker, M. Wiltberger, C. Goodrich, R. E. Lopez, and J.G. Lyon, Pseudobreakup and substorm onset: Observations and MHD simulations compared, *J. Geophys. Res., 103,* 14,847-14,854, 1998b.

Rostoker, G., Phenomenology and physics of magnetospheric substorms, *J. Geophys. Res., 101,* 12,955-12,973, 1996.

Rothwell, P. L., L. P. Block, M. B. Silevitch, and C.-G. Falthammar, A new model for substorms onsets: The pre-breakup and triggering regimes, *Geophys. Res. Lett., 15,* 1279-1282, 1988.

Russell, C. T., The control of the magnetopause by the interplanetary magnetic field. in *Dynamics of the Magnetosphere, Astrophys. Space Sci. Libr., vol. 78,* edited by S.-I. Akasofu, pp 3-21, D. Reidel Publ. Co., Norwell, Mass., 1980.

Russell, C. T. and R. L. McPherron, The magnetotail and substorms, *Space Sci. Rev., 15,* 205-266, 1973.

Schindler, K., D. N. Baker, J. Birn, E. W. Hones Jr., J. A. Slavin, and A. B. Galvin, *J. Geophys. Res., 94,* 15,177-15,188, 1989.

Scurry, L. and C. T. Russell, Proxy studies of energy transfer in the magnetosphere, Analysis of an extended period of earthward plasma sheet flow at ~ 220 R_E: CDAW 8, *J. Geophys. Res., 96,* 9541-9548, 1991.

Sergeev, V. A., T. I. Pulkkinen, and R. J. Pellinen, Coupled-mode scenario for the magnetospheric dynamics, *J. Geophys. Res., 101,* 13,047-13,065, 1996.

Slavin, J. A., E. J. Smith, D. J. Sibeck, D. N. Baker, R. D. Zwickl, and S.-I. Akasofu, An ISEE 3 study of average and substorm conditions in the distant magnetotails, *J. Geophys. Res., 90,* 10,875-10,895, 1985.

Sotirelis, T., P. T. Newell, and C.-I. Meng, Shape of the open-closed boundary of the polar cap as determined from observations of precipitating particles by up to four DMSP satellites, *J. Geophys. Res., 103,* 399-406, 1998.

Spiro, R. W., P. H. Reiff, and L. J. Maher Jr., Precipitating electron energy flux and auroral zone conductances: An empirical model, *J. Geophys. Res., 87,* 8215-8217, 1982.

Stern, D. P., and I. I. Alexeev, Where do field lines go in the quiet magnetosphere?, *Rev. Geophys., 26,* 782-791, 1988.

Zwickl, R. D., L. F. Bargatze, D. N. Baker, C. R. Clauer, and R. L. McPherron, An evaluation of the total magnetospheric energy output parameter, U_T, in *Magnetotail Physics,* edited A. T. Y. Lui, pp.155-159, Johns Hopkins Univ. Press, Baltimore, Md., 1987.

A. D. Bazarzhapov, V. M. Mishin, and T. I. Saifudinova, Institute of Solar-Terrestrial Physics, Russian Academy of Sciences, P.O.Box 4026 Irkutsk, 664033 Russia

C. T. Russell, Institute of Geophysics and Planetary Physics, 3845 Slichter Hall, University of California, Los Angeles, 405 Hilgard Avenue, Los Angeles, CA 90095-1567, (ctrussel@igpp.ucla.edu)

(Received December 12, 1997; revised September 16, 1999; accepted November 18, 1999.)